YMTHE, Volume *30*

Supplemental Information

Extracellular vesicle-mediated communication between hepatocytes and natural killer cells promotes hepatocellular tumorigenesis

Zhijun Liu, Yuyu You, Qiyi Chen, Guobang Li, Wenfeng Pan, Qing Yang, Jiajun Dong, Yi Wu, Jin-Xin Bei, Chaoyun Pan, Fuming Li, and Bo Li

Supplemental Figures

Figure S1

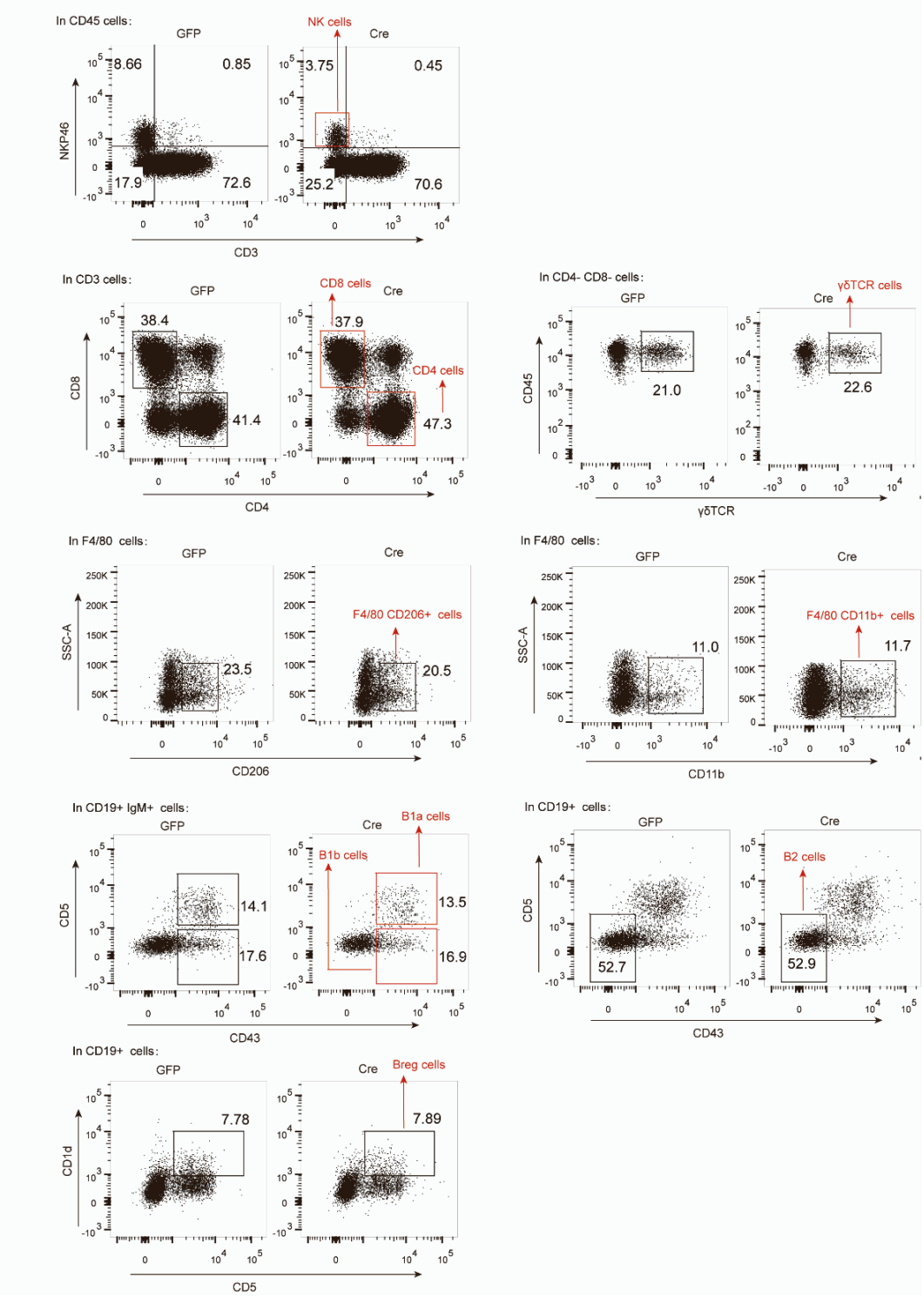

Figure S1. Gating strategy for leukocytes isolated from harvested tumor tissues in Figure 1.

Figure S2

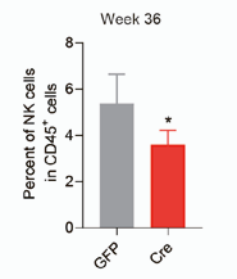

Figure S2. Hepatocyte-specific FBP1 loss restrains NK cells at 36 weeks in the DEN-treated Cre cohort compared to the control GFP cohort. Flow cytometry analysis of NK cell population in the liver tissues from DEN treated mice at Week 36 (n=6). Data represent mean ± SEM. Two-tailed unpaired t tests were performed to calculate P values. *P < 0.05.

Figure S3

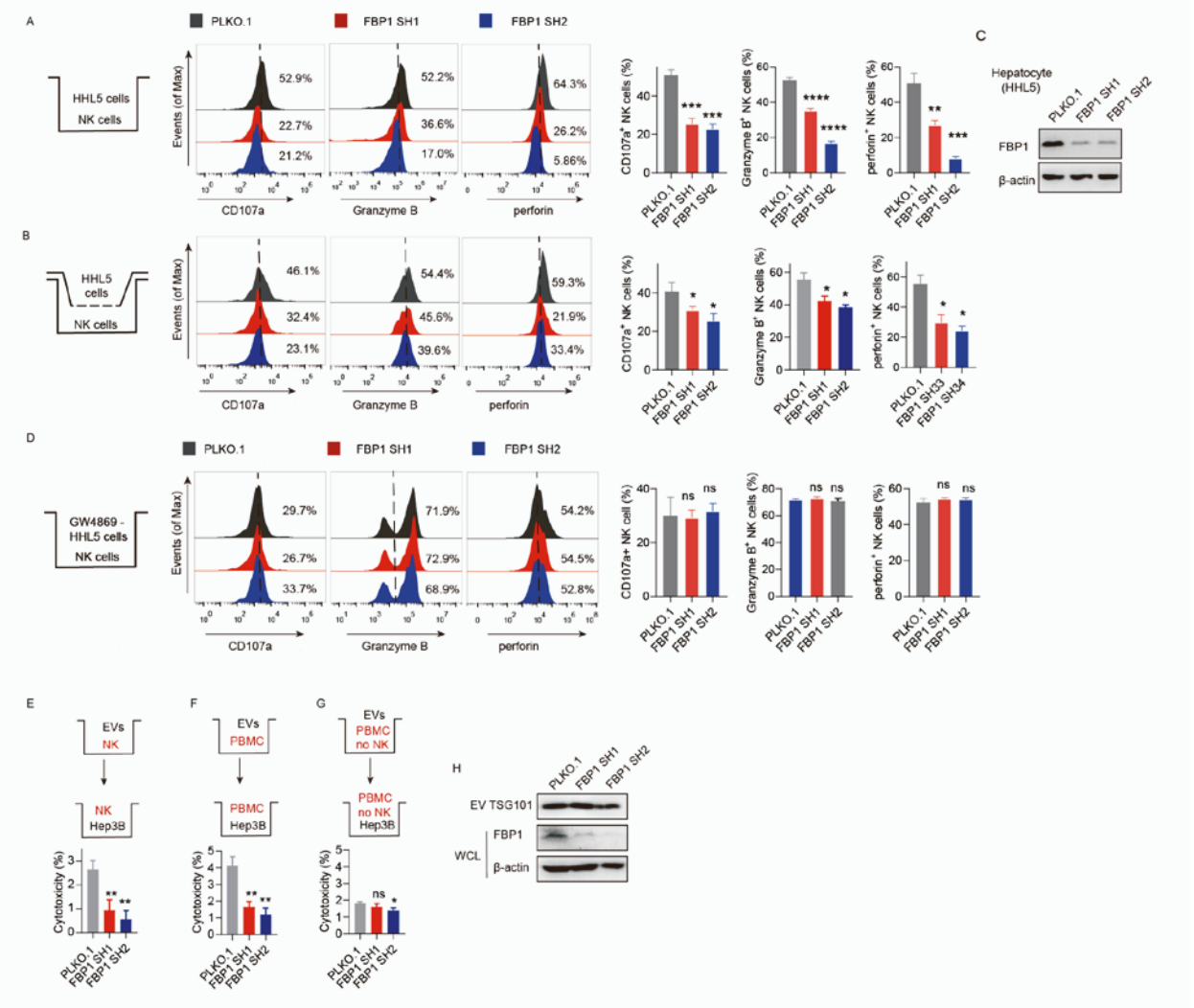

Figure S3. EVs secreted by FBP1-deficient hepatocytes impair NK cell function.

(A) Representative histograms (left) and quantifications (right) of indicated markers in NK cells. Flow cytometry analysis of NK cells directly co-cultured with hepatocytes with control PLKO.1 or FBP1 shRNAs.

(B) Representative histograms (left) and quantifications (right) of indicated activation markers in NK cells. Flow cytometry analysis of NK cells co-cultured with hepatocytes with control PLKO.1 or FBP1 shRNAs in a Transwell system.

(C) Western blots confirming the knockdown efficiencies of FBP1 shRNAs.

(D) Representative histograms (left) and quantifications (right) of indicated markers in NK cells directly co-

cultured with hepatocytes with control PLKO.1 or FBP1 shRNAs after GW4869 treatments.

(E-G) Cytotoxicity assays against Hep3B cells using NK cells (E), PBMCs (F) or NK-depleted PBMCs (G) cultured with EVs derived from hepatocytes with or without FBP1.

(H) Western blots confirming the knockdown efficiencies of FBP1 shRNAs.

Data represent mean ± SEM. Two-tailed unpaired t tests were performed to calculate P values. **P < 0.01; ***P < 0.001; ****P < 0.0001; ns, no significance.

Figure S4

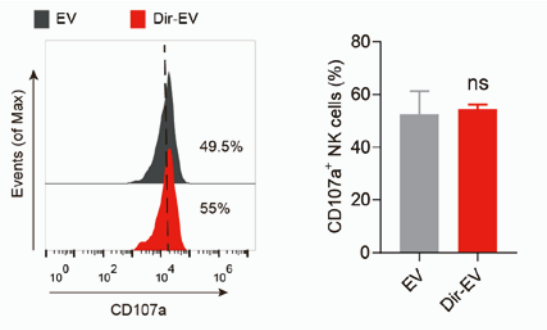

Figure S4. Dir staining fails to affect the EV activity.

FCS analysis of NK cells incubated with EVs with or without Dir staining. Representative histogram (left) and quantification (right) of $CD107a^+$ NK cells. Data represent mean ± SEM. Two-tailed unpaired t tests were performed to calculate P values. ns, no significance.

Figure S5

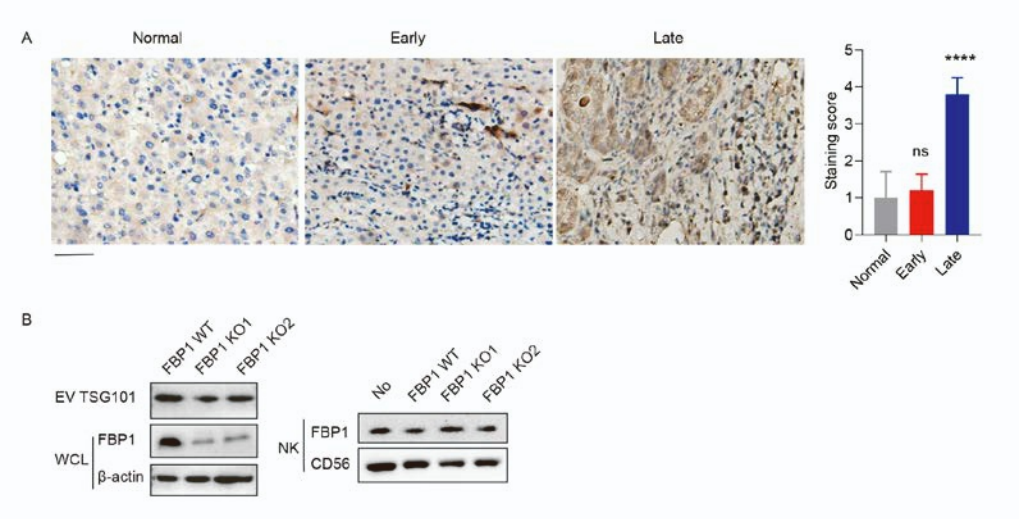

Figure S5. EVs secreted by hepatocytes with or without FBP1 depletion are unable to affect the endogenous FBP1 expression in NK cells, which are not regulated by TGF-β during tumorigenesis.

(A) Representative images (left) and quantifications (right) of TGF-β stainings in normal adjacent, early and late human HCC tissue sections. (scale bar, 50 μm).

(B) Western blotting confirming knockdown efficiencies of FBP1 by knockout clones in HHL5 cells and TSG101 expression in EVs (left). Western blotting assessing the FBP1 expression in NK cells incubated with EVs secreted from HHL5 cells containing normal or silenced FBP1 (right).

Figure S6

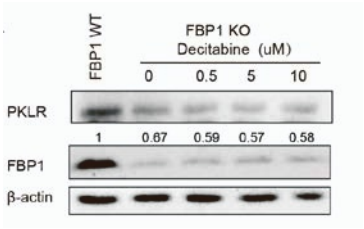

Figure S6. Decitabine fails to rescue the protein expression of PKLR in FBP1-depleted hepatocytes. Western blot analysis of FBP1 WT and KO HHL5 clones treated with the DNMT inhibitor Decitabine with indicated doses.

Figure S7

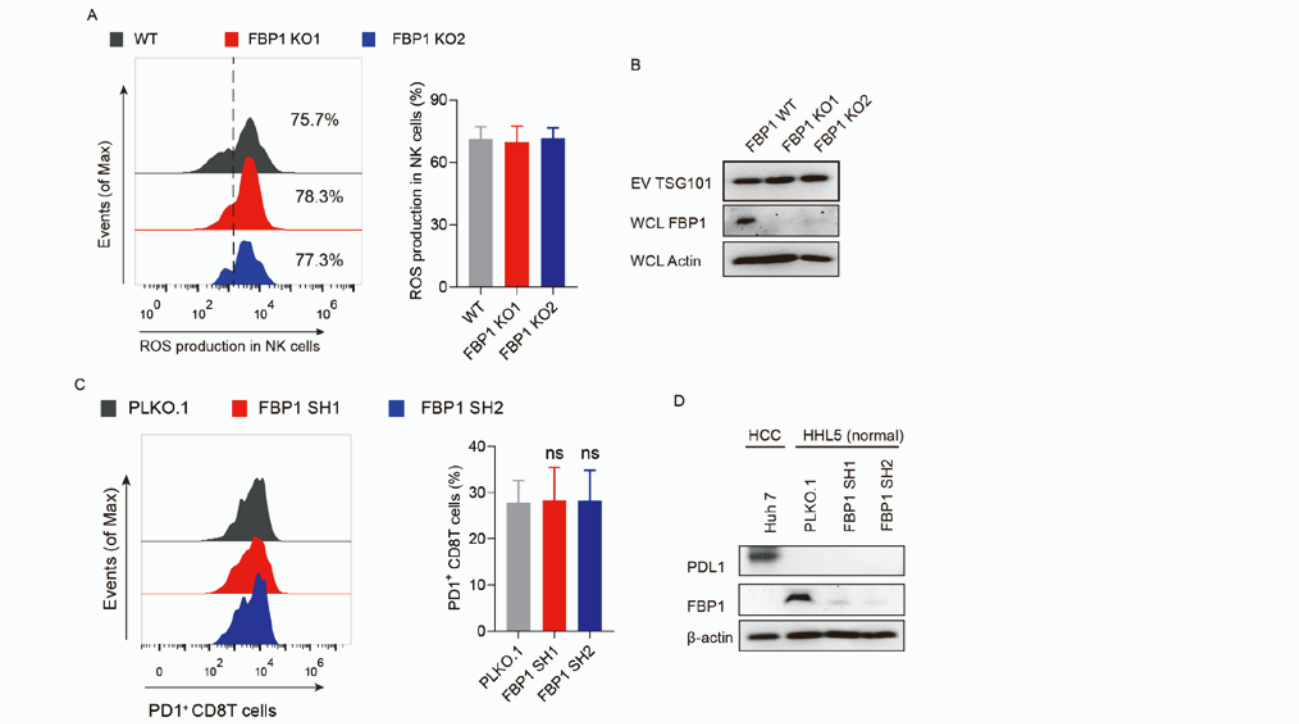

Figure S7. EVs secreted by hepatocytes with or without FBP1 does not affect the ROS levels of hepatic NK cells and exhausted CD8 T cells.

(A) ROS production in NK cells from mouse liver were assessed by flow cytometry analysis after tail vein injecting EVs secreted from indicated hepatocytes into C57BL/6 mice for 24h. The histograms (left) and quantification (right) of ROS production were shown.

(B) Western blotting confirming knockdown efficiencies of FBP1 by knockout clones in HHL5 cells and TSG101 expression in EVs.

(C) Exhausted CD8 T cells were analyzed by detecting $PD1^+$ CD8 T cells using flow cytometry. Hepa1-6 cells were inoculated as subcutaneous tumor grafts into C57BL/6 mice, and mice were treated with EVs secreted from Hepa1-6 cells with or without FBP1 through intratumoral injection two days a week until the endpoint.

(D) Western blotting of FBP1 and PD-L1 expression in HHL5 and Huh7 cells.

Figure S8

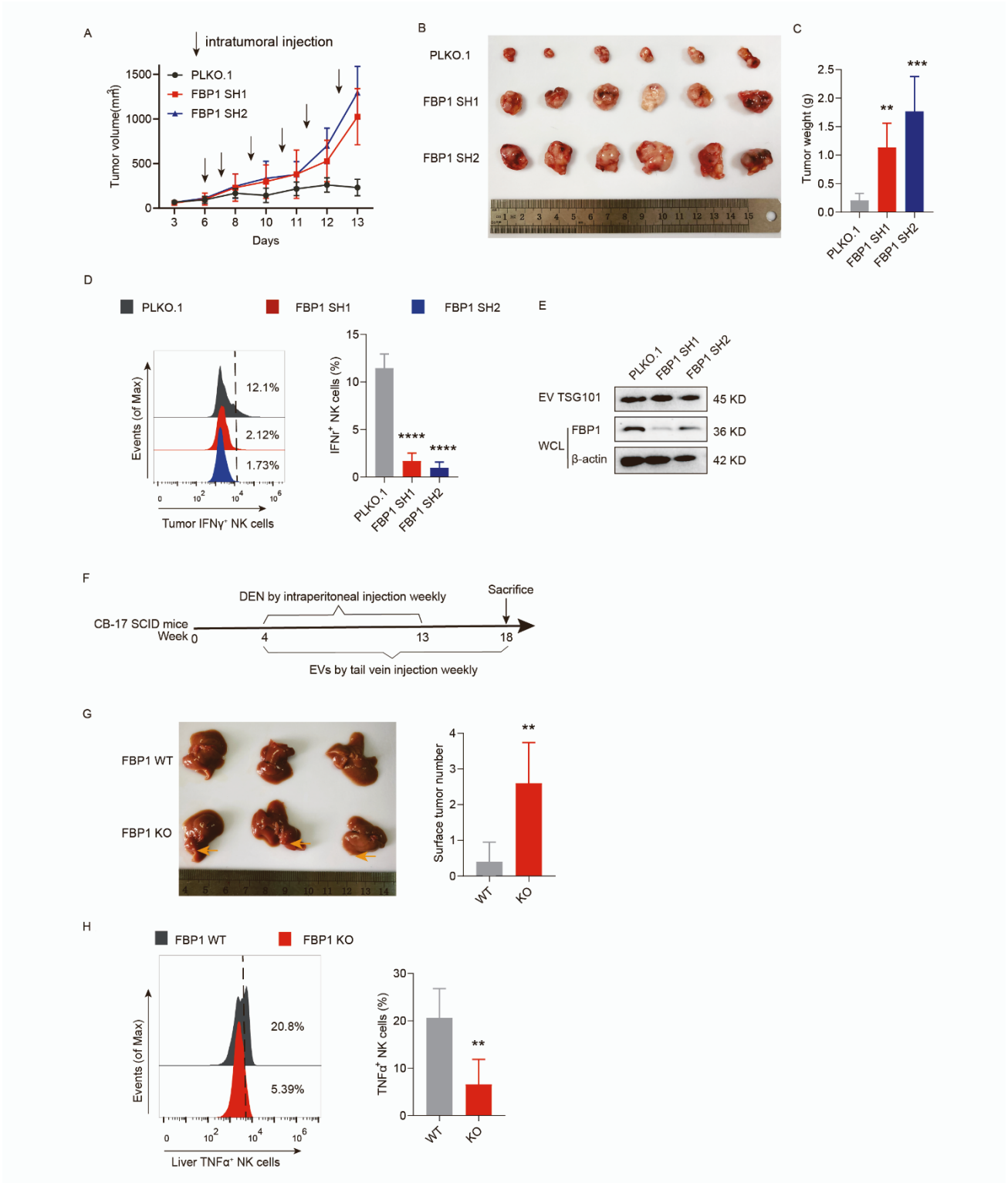

Figure S8. EVs secreted by FBP1-depleted liver cells accelerate tumor progression *in vivo*.

(A-C) Hepa1-6 cells were inoculated as subcutaneous allografts in C57BL/6 mice, which were treated with EVs

secreted from Hepa1-6 cells with or without FBP1 through intratumoral injection as indicated frequency until the endpoint. The volume growth of allograft tumors in mice was measured (A). The resulting tumor images (B) and weights (C) were shown.

(D) Representative histograms and quantifications of activated NK cells (IFN positive) in isolated tumors tissues, n=6.

(E) Western blot analysis of FBP1 and beta-actin expressions in WCL, and TSG101 expression in EVs secreted by Hepa1-6 cells.

(F) Experimental scheme examining the effect of hepatocyte-derived EVs in DEN-induced HCC model using the CB17-SCID immunocompromised mice.

(G) Representative images of whole livers (left) and the number of surface tumor nodules (right) in DEN-treated CB17-SCID mice after injecting EVs secreted by indicated clones, n=5.

(H) Representative histograms and quantifications of activated NK cells (TNFα positive) in aforementioned livers, n=5.

Figure S9

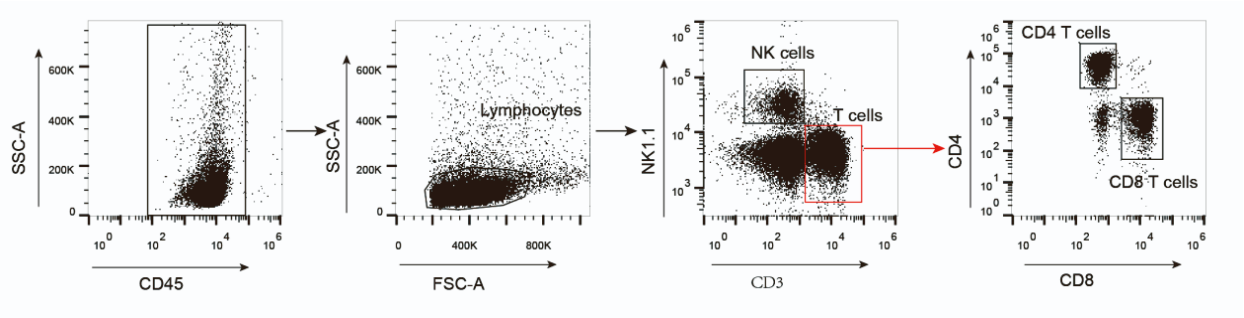

Figure S9. Gating strategy for leukocytes isolated from harvested tumor tissues in Figure 6.

Supplemental Tables

Table S1. Recognition sequences of shRNAs and sgRNAs.

shRNA or sgRNA	Recognition sequence (5' to 3')
EZH2 shRNA1	TATTGCCTTCTCACCAGCTGC
EZH2 shRNA2	CGGAAATCTTAAACCAAGAAT
PKLR shRNA1	GCATTGAAAGTGGAAAGCTCC
PKLR shRNA2	CCCACTGAGGTCACCGCCATT
FBP1 shRNA1	CCTTGATGGATCTTCCAACAT
FBP1 shRNA2	CGACCTGGTTATGAACATGTT
FBP1 sgRNA1	GGACACAAGGCAATCGATGT
FBP1 sgRNA2	GCCGTCACTGAGTACATCCAG
Mouse FBP1 shRNA1	CATAGCTTATGTCATGGAGAA
Mouse FBP1 shRNA2	CTACAGCCTTAATGAGGGTTA

Table S2. Sequences of primers used for RT-PCR and cloning.

Gene	Primer	Sequence (5' to 3')
PKLR 3-UTR-1	Forward	TCCCTACCTGAGGCCTATCTGAG
	Reverse	ACTGGGATTAAAGACTCAAGGCA
PKLR 3-UTR-2	Forward	AGCCTACCCTTGTACCCCAT
	Reverse	CAGGTAGGGAGGGTCAGGAA
PKLR 3-UTR-3	Forward	AATCTGGGCATCTCGTGCCA
	Reverse	AGCCAGGACAGTGGTCTACA
PKLR 3-UTR-4	Forward	CCTGCACCAACAGCAAACTC
	Reverse	TGAGAGAGGGAGAAGGACCG
PKLR CDS-1	Forward	TCAAGGCCGGGATGAACATTG
	Reverse	CTGAGTGGGGAACCTGCAAAG
PKLR CDS-2	Forward	GGACACGGCATCAAGATCATC
	Reverse	GCAGCGCCCAATCATCATC
GDF7	Forward	TCCAGCCTTAACGACGCAG
	Reverse	CAACGGCGGAGAAGTCCAG
PAX7	Forward	TCCAAGATTCTTTGCCGCTAC
	Reverse	GGTCACAGTGCCCATCCTTC
BMI1	Forward	CCACCTGATGTGTGTGCTTTG
	Reverse	TTCAGTAGTGGTCTGGTCTTGT
GAPDH	Forward	GGAGCGAGATCCCTCCAAAAT
	Reverse	GGCTGTTGTCATACTTCTCATGG
HOXA7	Forward	CGTTCCGGGCTTATACAATGT
	Reverse	CTCGTCCGTCTTGTCGCAG
HOXC13	Forward	GCCGTCTATACGGACATCCC
	Reverse	GGTAGGCGCAAGGCTTCTG
EPHB3	Forward	ATACCAGGTGTGTAATGTGCG
	Reverse	CGCTGTCAGCCTCGTAGTAG
DUOXA2	Forward	GCTGAACGAGACCATTGACTAC
	Reverse	CTCGGTGTGAACTTCTCCGC
OSR2	Forward	TCCGCCTAAGATGGGAGACC
	Reverse	GGTAAAGTGTCTGCCGCAAAA
DHH	Forward	CACCACGCTCAGGATTCACTC
	Reverse	CAACCCATACTTGTTGCGGTC
NUP210	Forward	ATGCCTTCCGATCAGTACGAG
	Reverse	CGACCACGTAGATAGTGCTGT
CDKN2C	Forward	GGGGACCTAGAGCAACTTACT
	Reverse	CAGCGCAGTCCTTCCAAAT
EGR3	Forward	GACATCGGTCTGACCAACGAG
	Reverse	GGCGAACTTTCCCAAGTAGGT
18S	Forward	CTACCACATCCAAGGAAGCA
	Reverse	TTTTTCGTCACTACCTCCCCG

Table S3. Antibodies used in flow cytometry analysis.

Antibodies used in flow cytometry	Source	Identifier
PE anti-human CD107a antibody	BioLegend	Cat#328608
APC anti-human CD56 antibody	BioLegend	Cat#318310
PE anti-human perforin antibody	BioLegend	Cat#308106
PE anti-human/mouse granzyme B antibody	BioLegend	Cat#372208
APC anti-human CD69 antibody	BioLegend	Cat#310910
FITC anti-human CD3 antibody	BioLegend	Cat#300406
Purified anti-mouse NK-1.1 Antibody	BioLegend	Cat#108702
Brilliant Violet 570™ anti-mouse CD45 antibody	BioLegend	Cat#103136
eFluor 450 anti-mouse IFN gamma antibody	Thermo Fisher Scientific	Cat#48-7311-8
PE-Cyanine7 CD4 antibody	eBioscience	Cat#25-0041-81
FITC anti-mouse CD8a antibody	eBioscience	Cat#11-0081-82
Alexa Fluor 700 anti-mouse CD3 antibody	eBioscience	Cat#56-0032-82
APC anti-mouse CD45R/B220 antibody	eBioscience	Cat#553091
APC anti-mouse TNF-α antibody	BioLegend	Cat#506307
PE anti-mouse NK1.1 antibody	BioLegend	Cat#108707
APC anti-mouse CD19 antibody	BD Biosciences	Cat#550992
APC-Cy7 anti-mouse CD4 antibody	BD Biosciences	Cat#552051
PE-Cy7 anti-mouse CD8a antibody	BD Biosciences	Cat#552877
FITC anti-mouse CD45 antibody	BD Biosciences	Cat#561088
V450 anti-mouse CD3e antibody	BD Biosciences	Cat#560801
PE-Cy7 anti-mouse CD45 antibody	BD Biosciences	Cat#552848
V450 anti-mouse CD11c antibody	BD Biosciences	Cat#560521
PE anti-mouse CD1d antibody	BD Biosciences	Cat#553846
APC anti-mouse CD5 antibody	BD Biosciences	Cat#561895
V450 anti-mouse CD19 antibody	BD Biosciences	Cat#560375
PerCP Cy™5.5 anti-mouse CD11b antibody	BD Biosciences	Cat#561114
PE anti-mouse γδ TCR antibody	Thermo Fisher Scientific	Cat#12-5711-82
PerCP-eFluor 710 anti-mouse NKp46 antibody	Thermo Fisher Scientific	Cat#46-3351-80
PE anti-mouse F4/80 antibody	Thermo Fisher Scientific	Cat#12-4801-82
FITC anti-mouse IgM antibody	BioLegend	Cat#406505
FITC anti-mouse CD206 antibody	Bio-Rad	Cat#MCA2235FT